Surface/interface-roughness-induced demagnetizing effect in thin magnetic films

Y.-P. Zhao
Department of Physics, Applied Physics, and Astronomy, and Center for Integrated Electronics and Electronics Manufacturing, Rensselaer Polytechnic Institute, Troy, New York 12180-3590

G. Palasantzas
Department of Applied Physics, Materials Science Center, University of Groningen, Nijenborgh 4, 9747 AG Groningen, The Netherlands

G.-C. Wang
Department of Physics, Applied Physics, and Astronomy, and Center for Integrated Electronics and Electronics Manufacturing, Rensselaer Polytechnic Institute, Troy, New York 12180-3590

J. Th. M. De Hosson
Department of Applied Physics, Materials Science Center, University of Groningen, Nijenborgh 4, 9747 AG Groningen, The Netherlands
(Received 3 December 1998; revised manuscript received 12 February 1999)

We study the influence of surface/interface roughness on the demagnetizing factor of a thin magnetic film with a single or a double boundary of self-affine, mound or anisotropic roughness. For a film with a single self-affine rough boundary, the in-plane demagnetizing factor $N_{xx(yy)}$ is proportional to the interface width w square and to the leading order is inversely proportional to the lateral correlation length ξ. The roughness exponent α is also shown to greatly affect $N_{xx(yy)}$. For a film with a single mound boundary, $N_{xx(yy)}$ is inversely proportional to the apparent correlation length, and also depends on the ratio of the two different lateral lengths: the average mound separation λ and the randomness correlation length ζ. It is also shown that an anisotropic surface morphology can induce anisotropic in-plane demagnetizing factors. The demagnetizing anisotropy can be magnified by a morphological anisotropy. Furthermore, we consider films with two rough boundaries. Besides a general formalism derived for the demagnetizing factor, we investigate how the cross correlation of the two rough boundaries affects the in-plane demagnetizing factors. Connections between the demagnetizing factor and thin-film growth mechanisms are also discussed. [S0163-1829(99)12125-8]

I. INTRODUCTION

Recently there has been a great interest on how surface roughness will affect the properties of thin magnetic films, such as coercivity, magnetic domain structure, magnetization reversal, and magnetoresistance.[1–4] These magnetic properties greatly affect the applications of thin magnetic films in magnetic recording industry, as well as other applications in magnetoelectronics. Many experiments have been performed for thin magnetic films with two kinds of rough boundaries. One kind is a film with a single rough boundary.[5–7] For example, Jiang *et al.* studied the relation of the coercivity versus surface roughness of Co ultrathin films deposited on an atomically flat Cu substrate.[5] Vilain *et al.* investigated the coercivity versus surface roughness of electrodeposited NiCo alloy films,[6] and Malyutin, *et al.* showed that the coercivity of chemically etched Ni-Fe-Co films increases with the surface roughness.[7] Very recently, Freeland *et al.* using the x-ray resonant magnetic scattering studied hysteretic behavior of CoFe thin films with varying roughness.[8] They also found the coercivity increased with the surface roughness. The other kind is a film with double rough boundaries.[5,9,10] Recently Li *et al.* performed a detailed study of thin Co films deposited on plasma etched Si(100) films.[9] They found that the uniaxial magnetic anisotropy decreases with the increase of surface roughness. Jiang *et al.* also investigated ultrathin Co films on an Ar^+-sputtered Cu substrate, and found that the coercivity increases with increasing surface roughness.[5] Kim *et al.* studied the underlayer Si_3N_4 roughness on the coercivity of the Co/Pt multilayers.[10] They also found that the coercivity enhanced with the increase of thickness (roughness) of the Si_3N_4 underlayer.

So far there are only a few theoretical examinations discussing the effects of surface/interface roughness on magnetic films.[11–13] This is probably due to the complicated nature of the problem. Physically, all magnetic properties are related to the magnetic energy of a thin film. Besides surface/interface roughness, many other factors such as film thickness, composition, crystalline structure of the magnetic film, magnetic domain distribution and correlation, contribute to the magnetic energy and determine the magnetization mechanism of a film. These are very important factors, and cannot be neglected in practice. However, in order to distinguish which factor dominates, each factor needs to be investigated individually. In this work, we concentrate on how surface/interface roughness affects the magnetic energy of a thin film, or alternatively, how boundary roughness influences the demagnetizing factor of a thin film.

In general, the demagnetizing field of a magnetic material is caused by the generation of ''magnetic poles'' near its boundaries due to the finite shape of a material. The magnetic poles give rise to a demagnetizing field $\mathbf{H}_d$, which is opposing the applied field. The strength of $\mathbf{H}_d$ depends on the geometry and the magnetization of a material $\mathbf{M}$:$\mathbf{H}_d$

$=\vec{\mathbf{N}}\cdot\mathbf{M}$, where $\vec{\mathbf{N}}$ is the demagnetizing tensor, depending on the shape of a magnetic object. For a smooth and infinite large thin magnetic film, its boundary in the film plane extends to infinity, and the demagnetizing factor in the film plane should be zero, but the demagnetizing factor along the out-of-plane direction of a thin film is nonzero. However, if the film is rough, the local roughness features will induce local in-plane ''magnetic poles,'' which may result in a nonzero in-plane demagnetizing factor. This problem was initially treated by Schlömann in the 1970s for a single sinusoidal rough boundary.[11] He found that the in-plane demagnetizing factor $N_{xx(yy)}\propto\Delta^2/\lambda$, where Δ and λ are the amplitude and the wavelength of the sinusoidal boundary, respectively. Recently, one of us (G.P.) extended this treatment to some special statistically rough self-affine surfaces[13] and found that $N_{xx(yy)}\propto w^2/\xi$ with w being the surface width and ξ being the in-plane roughness correlation length, as well as a strong dependence on the roughness exponent α of a surface. In general, surface roughness is determined by the thin-film deposition methods and conditions as well as the initial substrate roughness. Furthermore, the growth front of a thin film and the substrate roughness are closely related by the thin-film growth mechanism. A different surface morphology such as self-affine, mound or anisotropic surface can be formed from a different growth mechanism. Previous theoretical works[11,13] did not consider how these different kinds of morphology and especially the dynamics of growth mechanism will affect the demagnetizing factors. Experimentally it has been shown that substrate roughness can contribute strongly to the magnetic properties,[5,9,10] but the quantitative connection with theoretical result was not made.[11,13]

The organization of this paper is as follows: In Sec. II we derive a general formalism for the demagnetizing factor of thin films with rough boundaries. In Sec. III we consider the demagnetizing factor of a single rough boundary, where we investigate thoroughly how different surface morphologies affect this factor. In Sec. IV we investigate the cross-correlation effect of double rough boundaries by taking into account dynamic growth effects through linear Langevin growth models. In the end, we conclude our results.

II. DEMAGNETIZING FACTORS FOR MAGNETIC FILMS WITH ROUGH BOUNDARIES

The basic assumptions made here are that the film is uniform and single domain with a homogeneous magnetization $\mathbf{M}_0$ throughout the film. We assume the general case where the two interfaces of the magnetic film as shown in Fig. 1 are rough. These interfaces are described by the boundaries $d/2+h_1(\mathbf{r})$ and $-d/2+h_2(\mathbf{r})$, respectively, with $h_i(\mathbf{r})(i=1,2)$ being single-valued random surface height fluctuations. Here $\mathbf{r}=(x,y)$ is the in-plane position vector, and d is the average film thickness. The magnetization in a film can be written as

$$\mathbf{M}(\mathbf{x})=\mathbf{M}_0\left[\theta\left(z+\frac{d}{2}-h_2(\mathbf{r})\right)-\theta\left(z-\frac{d}{2}-h_1(\mathbf{r})\right)\right]$$

with $\mathbf{x}=(\mathbf{r},z)$ and $\theta(z)$ is a step function. According to Jackson,[14] for a uniform magnetization, the magnetic scalar potential can be written as

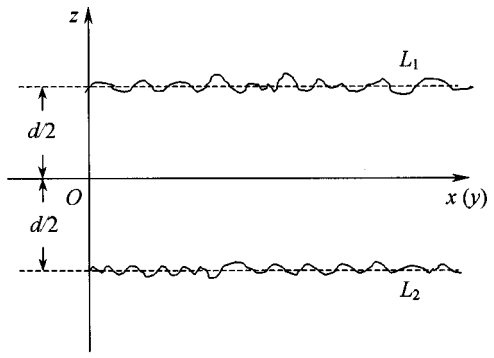

FIG. 1. A cross section of a rough film lying in the x-y plane. The growth front is in the z direction. The film thickness is d, with the boundaries L_1: $d/2+h_1(\mathbf{r})$ and L_2: $-d/2+h_2(\mathbf{r})$.

$$\begin{aligned}\Phi_M(\mathbf{x})&=\oint_s\frac{\hat{n}'\cdot\mathbf{M}(\mathbf{x}')}{|\mathbf{x}-\mathbf{x}'|}da'\\&=\int d\mathbf{r}'\frac{(\partial h_1/\partial x')M_{0x}+(\partial h_1/\partial y')M_{0y}-M_{0z}}{\sqrt{(\mathbf{r}-\mathbf{r}')^2+[z-d/2-h_1(\mathbf{r}')]^2}}\\&\quad-\int d\mathbf{r}'\frac{(\partial h_2/\partial x')M_{0x}+(\partial h_2/\partial y')M_{0y}-M_{0z}}{\sqrt{(\mathbf{r}-\mathbf{r}')^2+[z+d/2-h_2(\mathbf{r}')]^2}}.\end{aligned}\tag{1}$$

Note that $\hat{n}'$ is the surface normal pointing away from the surface, and da' is the differential surface area. According to Schlömann,[11] the self-energy can be written as

$$W=-\frac{1}{2}\int d\mathbf{r}\int dz\mathbf{H}\cdot\mathbf{M},\tag{2}$$

with the magnetic-field strength $\mathbf{H}=\nabla\Phi_M$. Substituting Eq. (1) into Eq. (2) (see Appendix A) we obtain the final expressions for the demagnetizing factors N_{xx}, N_{yy}, and N_{zz} in real space. Here N_{xx}, N_{yy}, and N_{zz} are the diagonal components of the demagnetizing tensor $\vec{\mathbf{N}}$. A similar calculation can be applied to the nondiagonal components N_{xy}, N_{yz}, and N_{zx}. To evaluate further the average in-plane demagnetizing factor, we consider the Fourier transform

$$\tilde{h}_i(\mathbf{k})=\frac{1}{(2\pi)^2}\int h_i(\mathbf{r})e^{i\mathbf{k}\cdot\mathbf{r}}d\mathbf{r},\tag{3}$$

$$h_i(\mathbf{r})=\int\tilde{h}_i(\mathbf{k})e^{-i\mathbf{k}\cdot\mathbf{r}}d\mathbf{k},\tag{4}$$

and assume a translation invariant surface/interface:

$$\langle\tilde{h}_i(\mathbf{k})\tilde{h}_j(\mathbf{k}')\rangle=\frac{(2\pi)^4}{A}\langle\tilde{h}_i(\mathbf{k})\tilde{h}_j(-\mathbf{k})\rangle\delta(\mathbf{k}+\mathbf{k}'),\tag{5}$$

where i, $j=1$, 2; and $\langle\,\rangle$ denotes an average over all possible choices of origins and an ensemble average over all possible surface configurations. Upon substitution, we obtain the ensemble average which finally yields

$$N_{xx} \approx \frac{(2\pi)^4}{2dA} \int d\mathbf{k} \frac{k_x^2}{k} [\langle |\tilde{h}_1(\mathbf{k})|^2 \rangle + \langle |\tilde{h}_2(\mathbf{k})|^2 \rangle - 2e^{-dk} \langle \tilde{h}_1(\mathbf{k}) \tilde{h}_2(-\mathbf{k}) \rangle]. \quad (6)$$

A similar expression for N_{yy} can be obtained. N_{zz} can be calculated from the orthogonality condition $N_{zz}=1-N_{yy}-N_{xx}$.[11] Equation (6) is the basic formula that we will study in this paper. However, we should emphasize that the assumption for Eq. (6) is that $w \ll d$, and the average local slope is also much less than one.

III. DEMAGNETIZING FACTORS FOR MAGNETIC FILMS WITH SINGLE ROUGH BOUNDARY

Magnetic thin-film growth usually commences on a very smooth surface. In this case $h_2=0$, we may simplify Eq. (6) to the form[11,13]

$$N_{xx} \approx \frac{(2\pi)^4}{2dA} \int d\mathbf{k} \frac{k_x^2}{k} \langle |\tilde{h}_1(\mathbf{k})|^2 \rangle, \quad (7)$$

which is actually the formula obtained by Schlömann.[11] However, Schlömann only considered the case for a sinusoidal rough interface, which may not occur in reality. In fact, due to the inherent noise during growth, the growth front of a thin film is statistically rough for the majority of cases. Under different preparation conditions (substrate temperature, pressure, growth rate), or different growth methods (physical vapor evaporation, sputtering, chemical vapor deposition, etc.), one may obtain a wide variety of different surface morphologies which are inherently related to different growth mechanisms.

So far, there are three kinds of statistical rough surfaces obtained in thin-film growth (1) *Self-affine surface:* This kind of surface usually results from the pure noise driven mechanism,[15] and one needs three parameters to characterize the surface, the interface width w, the lateral correlation length ξ, and the roughness exponent α. (2) *Mound surface:* If the surface has a diffusion barrier or has both smoothening and roughening mechanisms, then a mound surface is obtained.[16–18] For this kind of surface, there are two lateral length scales that characterize the morphology, namely the average mound separation λ and the randomness correlation length ζ.[18] (3) *Anisotropic surface:* if the substrate has an anisotropy, the growth front can be anisotropic. Recently Zhao *et al.* showed that when growth starts from a smooth substrate, if different growth mechanisms govern different growth directions, one could also obtain an anisotropic surface.[19,20] An intuitive question to ask is to what extent a morphological anisotropy will induce a magnetic anisotropy. Since there are two different kinds of anisotropy: lateral length anisotropy and scaling anisotropy,[20] it is important to investigate how they would affect the demagnetizing factor. In the following, we shall consider the effects of these statistical rough surfaces on the demagnetizing factors.

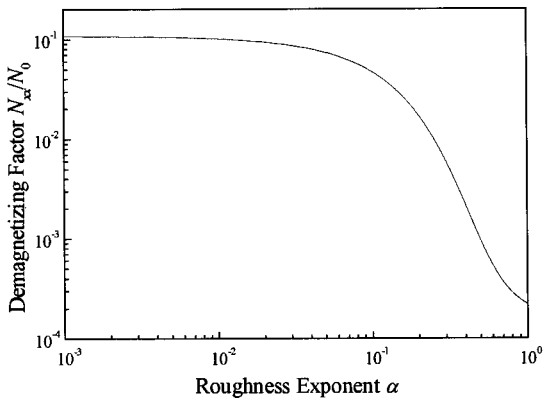

FIG. 2. Log-log plot of the in-plane demagnetizing factor N_{xx}/N_0 as a function of the roughness exponent α for an isotropic self-affine surface. Here $N_0=w^2/d\xi$.

A. Isotropic self-affine surface

In this case, one has[19–21]

$$\langle |\tilde{h}(\mathbf{k})|^2 \rangle = \frac{A}{(2\pi)^5} \frac{\alpha \xi^2 w^2}{(1+\xi^2 k^2)^{1+\alpha}}. \quad (8)$$

Here, w is the interface width describing the fluctuation of the surface height. ξ is the lateral correlation length within which the surface heights of any two points are correlated. The roughness exponent α ($0<\alpha<1$) describes how wiggly the surface is. Due to the isotropy $N_{xx}=N_{yy}$. Substituting Eq. (8) into Eq. (7) we can obtain N_{xx} as[22]

$$N_{xx} \approx \frac{\alpha w^2}{2d\xi} \left\{ 2^{-\alpha-1/2} \sqrt{\pi} \Gamma(1-\alpha) (\xi k_c)^{1/2-\alpha} \left[\mathbf{H}_{1/2-\alpha}\left(\frac{\alpha}{\xi k_c}\right) - Y_{1/2-\alpha}\left(\frac{\alpha}{\xi k_c}\right) \right] - 2^{-\alpha+1/2} \sqrt{\pi} \Gamma(-\alpha) (\xi k_c)^{-1/2-\alpha} \times \left[\mathbf{H}_{-1/2-\alpha}\left(\frac{\alpha+1}{\xi k_c}\right) - Y_{-1/2-\alpha}\left(\frac{\alpha+1}{\xi k_c}\right) \right] \right\}, \quad (9)$$

where $\mathbf{H}_v(x)$ is the Struve function and $Y_v(x)$ is the Neumann function, k_c is the upper spatial frequency boundary. Note that we assume the statistics is enough that it covers the entire scaling region. This assumption is made through out the whole paper and will not be stated again. Obviously for any self-affine surface, the in-plane demagnetizing factor to its leading order scales as $N_{xx(yy)} \propto w^2/d\xi$. This result is similar to that obtained in Refs. 11 and 13. Figure 2 shows how the roughness exponent α affects the demagnetizing factor. As α increases from 0.001 to 1, the in-plane demagnetizing factor decreases almost three orders of magnitude. The dependence of the demagnetizing factor on the roughness exponent α can be understood in the following: the roughness exponent α essentially represents how much high spatial frequency surface components are included in the surface. As α approaches from 1 to 0 (from the smooth facet to the more wiggly local slope variation), more and more high-frequency components are included in the power spectrum, which means that the surface has more small features of local variations. This will generate more ''magnetic poles'' on the surface parallel to the film plane, and will give rise to a stronger in-plane demagnetizing field. In fact, this result is

consistent with Schlömann's derivation that higher frequency component will contribute more to the demagnetizing factor.[11] Therefore, as α decreases, N_{xx} should increase.

For a self-affine growth on flat substrates, the dynamic scaling hypothesis can be assumed which states that $w \propto t^{\beta}$, and $\xi \propto t^{1/z}$, with β being the growth exponent and z being the dynamic exponent such that $z=\alpha/\beta$.[15] Thus, for linear growth ($d \propto t$) we obtain to the leading order the temporal variation of the lateral demagnetizing factor $N_{xx} \propto t^{2\beta-\beta/\alpha-1}$. For example, if the growth is governed by the surface diffusion, $\alpha=1$ and $\beta=1/4$ which gives $N_{xx} \propto t^{-3/4}$, i.e., with the increase of the growth time the demagnetizing factor caused by surface roughness diminishes.

B. Isotropic mound surface

In this case, one has[18]

$$\langle |\tilde{h}(\mathbf{k})|^2 \rangle = \frac{A}{(2\pi)^5} \frac{\zeta^2 w^2}{2} \exp\left(-\frac{4\pi^2 + k^2\lambda^2}{4\lambda^2} \zeta^2 \right) I_0\left(\frac{\pi \zeta^2 k}{\lambda} \right), \tag{10}$$

where λ is the average mound separation, ζ is the randomness correlation length, and $I_0(x)$ is the zeroth-order modified Bessel function. The in-plane demagnetizing factor can be written as

$$N_{xx} \approx \frac{\alpha w^2}{2d} \int \frac{\zeta^2 w^2 k^2}{2} \exp\left(-\frac{4\pi^2 + k^2\lambda^2}{4\lambda^2} \zeta^2 \right) I_0\left(\frac{\pi \zeta^2 k}{\lambda} \right) dk$$
$$= \frac{4w^2}{d\xi} \Gamma\begin{bmatrix} 3/2 \\ 1 \end{bmatrix} \exp\left(-\frac{\pi^2 \zeta^2}{\lambda^2} \right) M\left(\frac{3}{2}; 1; \frac{\pi^2 \zeta^2}{\lambda^2} \right), \tag{11}$$

with the Kummer's function $M(p;q;x)$. In this case, the apparent lateral correlation length ξ is a function of both ζ and λ:[18] $1/\xi^2 = (1/\zeta^2) + (\pi^2/\lambda^2)$. If we assume a fixed value of the apparent correlation length ξ, then one can introduce a dummy angle ϕ such that $1/\zeta^2 = (1/\xi^2)\cos^2\phi$, $\pi^2/\lambda^2 = (1/\xi^2)\sin^2\phi$, and the demagnetizing factor can be rewritten as

$$N_{xx} \approx \frac{8w^2}{d\xi} \Gamma\begin{bmatrix} 3/2 \\ 1 \end{bmatrix} \frac{1}{\sqrt{1+\gamma^2}} \exp(-\gamma^2) M\left(\frac{3}{2}; 1; \gamma^2 \right), \tag{12}$$

with $\gamma = |\tan\phi| = \pi\zeta/\lambda$ representing the ratio of the randomness correlation length to the average mound separation. Equation (12) clearly states that the demagnetizing factor is still inversely proportional to the lateral correlation length, and obeys the relation $N_{xx} \propto w^2/d\xi$. Moreover, from Eq. (12) we can see that for the mound surface, even for the same lateral correlation, the demagnetizing factor depends also on the ratio γ.

Figure 3 shows the demagnetizing factor N_{xx}/N_0 as a function of the ratio γ for a fixed $\xi=10$, and $N_0' = (8w^2/d\xi)\Gamma\left[{}^{3/2}_{1}\right]$. N_{xx} increases with increasing γ which means that ζ will contribute significantly to the demagnetizing factor. In general the formation of a mound surface is the result of the competition between roughening and smoothening growth mechanisms. Eventually, for a long time, the roughening mechanism will dominate, which suggests that the interface width w may increase exponentially with time while the film thickness still grows linearly. One example is the early stage equation of growth that describes the mound formation.[18] On the other hand, the average local slope w/ξ may remain unchanged due to the slope selection.[16] Therefore, the in-plane demagnetizing factor may increase with growth time as $N_{xx} \propto w^2/d\xi \propto e^{pt}/t$, or at least maintains a constant if $w \propto t$. In addition, as time increases, the ratio γ becomes smaller and the dominated correlation length will be the average mound separation λ. Note, however that, if the interface width grows exponentially, the condition $w/d \ll 1$ required for the validity of the in-plane demagnetizing factor expansion may not be satisfied for any film thickness d.

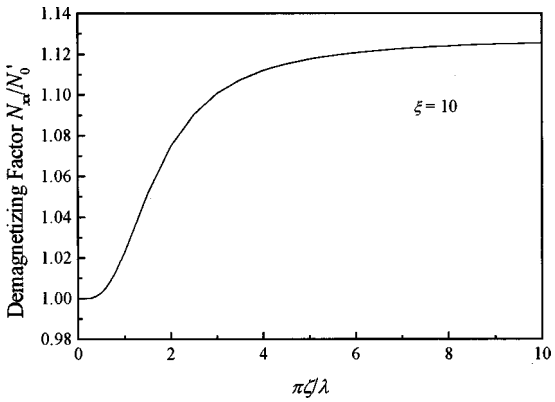

FIG. 3. In-plane demagnetizing factor N_{xx}/N_0 as a function of the lateral ratio $\pi\zeta/\lambda$ for a mound surface with a fixed apparent lateral correlation length ξ.

C. Anisotropic self-affine surface

Correlation length anisotropy: First we consider the lateral anisotropy case where one has[20]

$$\langle |\tilde{h}(\mathbf{k})|^2 \rangle = \frac{A}{(2\pi)^5} \frac{2\alpha \xi_x \xi_y w^2}{(1 + \xi_x^2 k_x^2 + \xi_y^2 k_y^2)^{1+\alpha}}, \tag{13}$$

with ξ_x and ξ_y being the correlation lengths in the x and y axes, respectively. From Eq. (13) we obtain the demagnetizing factor

$$N_{xx} \approx \frac{\alpha \xi_x \xi_y w^2}{\pi d} \int_0^{2\pi} d\theta \int_0^{k_c} \times \frac{k^2 \cos^2\theta}{(1 + \xi_x^2 k^2 \cos^2\theta + \xi_y^2 k^2 \sin^2\theta)^{1+\alpha}} dk. \tag{14}$$

Here we have changed the coordinates to cylindrical. If we consider $k_c \to \infty$ and $0.5 < \alpha < 1$, and consider the integral $I(x,y) = \int_0^{2\pi} (x\cos^2\theta + y\sin^2\theta)^{-1/2} d\theta$, we obtain

$$\xi_x^2 N_{xx} + \xi_y^2 N_{yy} = \frac{\sqrt{\pi} \xi_x \xi_y w^2 \Gamma(\alpha - 1/2)}{4\pi d \Gamma(\alpha)} I(\xi_x^2, \xi_y^2), \tag{15}$$

$$N_{xx} + N_{yy} = -\frac{\sqrt{\pi} \xi_x \xi_y w^2 \Gamma(\alpha - 1/2)}{2\pi d \Gamma(\alpha)} \left[\frac{\partial}{\partial x} + \frac{\partial}{\partial y} \right] I(\xi_x^2, \xi_y^2). \tag{16}$$

Where $I(x,y)$ can be reduced to an elliptic integral. Equations (15) and (16) show that the demagnetizing factor has the same relation for the roughness exponent as for the iso-

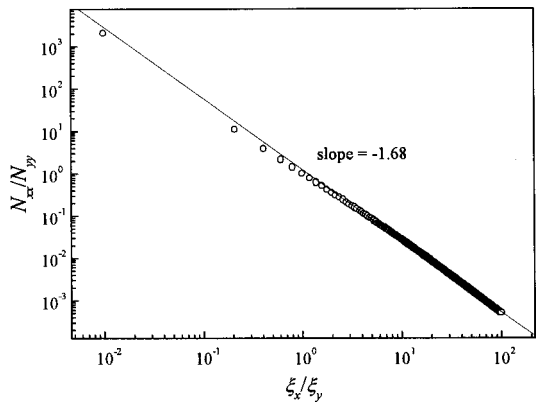

FIG. 4. Log-log plot of the ratio of in-plane demagnetizing factors N_{xx}/N_{yy} as a function of the lateral correlation length ratio ξ_x/ξ_y for a lateral length anisotropic surface. Note that in this case the ratio N_{xx}/N_{yy} does not depend on the roughness exponent α.

tropic self-affine surface with the relation $N_{xx(yy)} \propto w^2/d$ still valid. Figure 4 shows N_{xx}/N_{yy} as a function of the ratio ξ_x/ξ_y where the anisotropy of in-plane demagnetizing effect appears to rotate by 90° with respect to the surface morphology anisotropy. The in-plane demagnetizing factor anisotropy and the lateral length scale anisotropy obey the relation $N_{xx}/N_{yy} \propto (\xi_x/\xi_y)^{-1.7}$. This result implies that the slight anisotropy of surface morphology will amplify the in-plane demagnetizing effect. Therefore, such a result indicates that surface morphology anisotropy will have a great impact on the anisotropy of the magnetic properties. We demonstrated recently that the lateral length anisotropic surface is caused by the same growth mechanism but with different strength in the x and y directions.[19] Therefore, during growth, although both w and $\xi_{x(y)}$ are functions of growth time, the anisotropy ratio does not change temporally. As a result the anisotropy of the demagnetizing factor will not change during the deposition process.

Correlation length and scaling exponent anisotropy: Finally, in the case of the additional scaling anisotropy in roughness exponents, we have[20]

$$\langle |\tilde{h}(\mathbf{k})^2| \rangle = \frac{A}{(2\pi)^5} \frac{2\xi_x \xi_y w^2 \Gamma(1/2+\alpha_x)\Gamma(1/2+\alpha_y)}{(1+\xi_x^2 k_x^2)^{1/2+\alpha_x}(1+\xi_y^2 k_y^2)^{1/2+\alpha_y}}, \tag{17}$$

with α_x and α_y being the roughness exponents along the x and y axes, respectively. Therefore, we obtain

$$N_{xx} \approx \frac{\xi_x \xi_y w^2 \Gamma(1/2+\alpha_x)\Gamma(1/2+\alpha_y)}{\pi d} \int_0^{2\pi} d\theta \int_0^{k_c} \times \frac{k^2 \cos^2\theta}{(1+\xi_x^2 k^2 \cos^2\theta)^{1/2+\alpha_x}(1+\xi_y^2 k^2 \sin^2\theta)^{1/2+\alpha_y}} dk. \tag{18}$$

It was discussed in Ref. 20, for a scaling anisotropy surface, the anisotropy is determined by the lateral correlation lengths ξ_x, ξ_y, and also the roughness exponents α_x, α_y. Figure 5 shows the numerically calculated N_{xx} and N_{yy} as functions of α_x for fixed α_y: $\alpha_y = 1$ and $\alpha_y = 0.5$. Here $\xi_x = \xi_y = 50$ nm, $w = 1.0$ nm, and $d = 40$ nm, respectively. The intersection of N_{xx} and N_{yy} curves show that $N_{xx} = N_{yy}$ only at

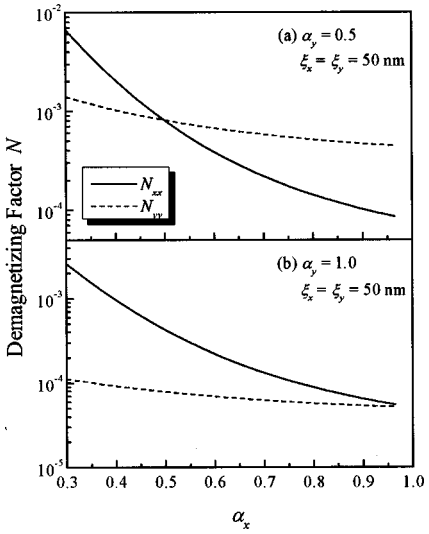

FIG. 5. Semilog-log plot of the in-plane demagnetizing factors N_{xx} and N_{yy} as functions of α_x for a scaling anisotropic surface. Here $\xi_x = \xi_y = 50$ nm and α_y is fixed for (a) $\alpha_y = 0.5$, and (b) $\alpha_y = 1.0$.

$\alpha_x = \alpha_y$, while for $\alpha_x < \alpha_y$ we have $N_{xx} > N_{yy}$ and vice versa. Moreover, Fig. 6 shows how the general anisotropy affects the in-plane demagnetizing factors for $\xi_x = 150$ nm, $\xi_y = 50$ nm, $\alpha_y = 0.5$; and $\xi_x = 50$ nm, $\xi_y = 150$ nm, $\alpha_y = 0.5$. Obviously, for $\xi_x > \xi_y$, the intersection of N_{xx} and N_{yy} curves shifts to smaller α_x, while for $\xi_x < \xi_y$, the intersection shifts to larger α_x.

IV. MAGNETIC FILMS WITH DOUBLE ROUGH BOUNDARIES

In this section we concentrate on how the cross correlation of the two rough boundaries affects the demagnetizing factors. For simplicity we will consider only isotropic rough boundaries. In this case $N_{xx} = N_{yy}$, and N_{xx} can be expressed as

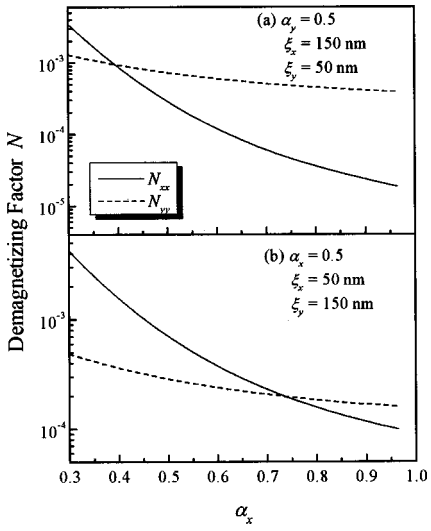

FIG. 6. Semilog-log plot of in-plane demagnetizing factors N_{xx} and N_{yy} as functions of α_x for a scaling anisotropic surface. Here $\alpha_y = 0.5$ is fixed for (a) $\xi_x = 3\xi_y = 150$ nm, and (b) $3\xi_x = \xi_y = 150$ nm.

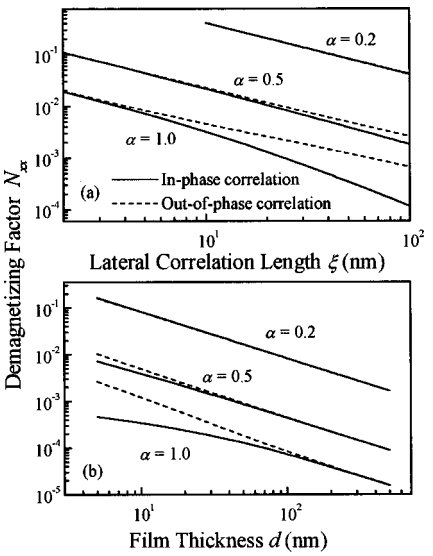

FIG. 7. Log-log plot of the demagnetizing factor N_{xx} as a function of (a) the lateral correlation length ξ with $w=1.0$ nm, $d=10$ nm, and (b) film thickness d with $w=1.0$ nm, $\xi=20$ nm for an in-phase cross-correlation and an out-of-phase cross-correlation.

$$N_{xx} \approx \frac{(2\pi)^5}{2dA} \int dk k^2 [\langle |\tilde{h}_1(\mathbf{k})|^2 \rangle + \langle |\tilde{h}_2(\mathbf{k})|^2 \rangle - 2e^{-2dk} \langle \tilde{h}_1(\mathbf{k}) \tilde{h}_2(-\mathbf{k}) \rangle]. \quad (19)$$

Effects of in-phase and out-of-phase boundaries: First, we consider a simple case in which $h_1 = \pm h_2$, i.e., the two rough boundaries are totally correlated: the positive sign and the negative sign represent the surfaces which are exactly in-phase and exactly out-of-phase, respectively. The in-plane demagnetizing factor can be written as

$$N_{xx} \approx \frac{\alpha w^2}{2d} \int_0^{k_c} \frac{\xi^2 k^2 (1 \mp e^{-2dk})}{(1+\xi^2 k^2)^{1+\alpha}} dk. \quad (20)$$

In Fig. 7 we plot the demagnetizing factor N_{xx} as functions of both the lateral correlation length ξ with $w=1.0$ nm, $d=10$ nm, and film thickness d with $w=1$ nm, $\xi=20$ nm for an in-phase cross correlation and an out-of-phase cross correlation, respectively. Clearly the demagnetizing factor of the in-phase boundaries is less than that of the out-of-phase boundaries. N_{xx} still decreases monotonically with increasing both the lateral correlation length ξ and film thickness d. However, for large roughness exponents $\alpha(=1)$, the demagnetizing factor N_{xx} for the in-phase boundaries is significantly smaller than that for the out-of-phase boundaries as ξ increases for a fixed film thickness, see Fig. 7(a) or as d decreases for a fixed ξ, see Fig. 7(b). Moreover, both the behaviors of N_{xx} versus ξ and N_{xx} versus d for the in-phase boundaries obviously deviates from the inversely proportional behavior with film thickness. Quantitatively, for the out-of-phase boundaries $N_{xx} \propto \xi^{-0.85}$ and $N_{xx} \propto d^{-1.1}$. As the value of the roughness exponent α decreases, the N_{xx} vs ξ and N_{xx} vs d behaviors for both the in-phase and out-of-phase boundaries becomes similar. N_{xx} overlap with each other for small exponents α and the inverse dependence over the lateral correlation length ξ, $N_{xx} \propto \xi^{-1}$, and film thickness d, $N_{xx} \propto d^{-1}$ recover.

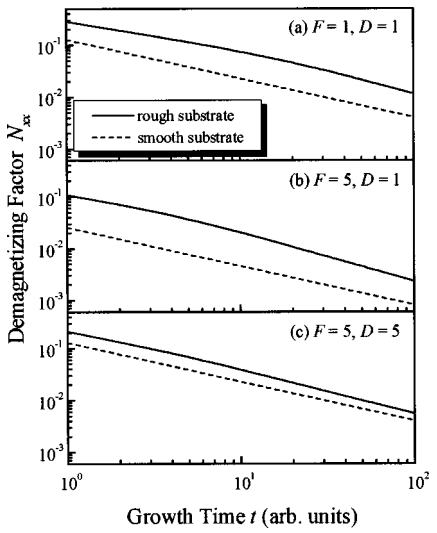

FIG. 8. Log-log plot of the N_{xx} as a function of growth time for a self-affine rough substrate with $\alpha=1$, $w=5$, $\xi=20$ for different F and D values: (a) $F=1.0$, $D=1.0$; (b) $F=5.0$, $D=1.0$; and (c) $F=5.0$, $D=5.0$.

Dynamic growth effects: In the following we consider how the dynamic growth will affect the demagnetizing factor. Since the growth starts from a rough substrate initially, the cross-correlation coefficient between the growth front and the substrate is positive, but less than 1, as shown in the Appendix B. Therefore, the ultimate effect of the cross correlation is to reduce the demagnetizing factor. A simple case is to consider the linear dynamic growth as shown in Eqs. (B8) and (B9) in Appendix B, where the in-plane demagnetizing factor can be written as

$$N_{xx} \approx \frac{1}{2Ft} \int dk k^2 \left[\langle |\tilde{h}_2(\mathbf{k})|^2 \rangle (1 - 2e^{-Fkt} e^{(\mp \nu k^2 - \kappa k^4)t} + e^{2(\mp \nu k^2 - \kappa k^4)t}) + D \frac{e^{2(\mp \nu k^2 - \kappa k^4)t} - 1}{\mp \nu k^2 - \kappa k^4} \right]. \quad (21)$$

For the linear dynamic growth equation shown in Appendix B, $d=Ft$ with F being the film growth rate. Here we have $Ft \gg w_1(t)$ in order to satisfy the perturbation condition. Equation (21) shows that the substrate effect decreases at least according to t^{-1}, but the effect of the growth front is determined by the growth mechanism. According to the discussion in Sec. III A, for a dynamic scaling growth front, the change of N_{xx} caused by this front evolved as $t^{2\beta-\beta/\alpha-1}$ where usually $1+\beta/\alpha-2\beta<1$. Therefore, after a certain time, the change of demagnetizing factor N_{xx} is dominated by the surface roughness contribution. Figure 8 plots the N_{xx} as a function of the growth time t for the Mullin's diffusion growth mechanism starting from a rough surface with $\alpha=1$, $w=5$, $\xi=20$ for different F and D values: (a) $F=1.0$, $D=1.0$; (b) $F=5.0$, $D=1.0$; and (c) $F=5.0$, $D=5.0$. Under the same growth mechanism we also plot the N_{xx} as a function of the growth time t starting from a smooth surface. One can see that as F increases, N_{xx} decreases, and the difference of N_{xx} between the rough substrate and smooth substrate becomes large. As D increases, the difference of N_{xx} between the rough substrate and smooth substrate becomes

small, and N_{xx} increases. Initially, the behavior of N_{xx} versus growth time t is greatly influenced by the substrate roughness, as shown in Fig. 8 the N_{xx} versus time for a rough substrate does not parallel that of a smooth substrate. However, after a long time, the surface growth dominates N_{xx}. The change of substrate morphology also affects the determination of the relationship N_{xx} versus t. If the substrate has a very long correlation length compared to its interface width, then the substrate almost has no effect on the time behavior of N_{xx}. The change of the substrate roughness exponent α also affects the absolute value of N_{xx}, but not as dramatic as the affect of the surface roughness exponent as discussed in Sec. III A.

V. DISCUSSIONS OF THE RESULTS IN CONNECTION WITH EXPIREMENTS

As we discussed above, the demagnetizing field changes the field strength inside the magnetic material. The magnetic field inside the material can be written as $\mathbf{H}=\mathbf{H}_{\rm app}-\mathbf{H}_d=\mathbf{H}_{\rm app}-\vec{\mathbf{N}}\cdot\mathbf{M}$. For an isotropic surface, one can prove that the nondiagonal components N_{xy}, N_{yz}, and N_{zx} of the demagnetizing tensor $\vec{\mathbf{N}}$ are equal to zero. The actual demagnetizing field depends on the diagonal components N_{xx}, N_{yy}, and N_{zz} of $\vec{\mathbf{N}}$, that is

$$H_x=H_{{\rm app},x}-N_{xx}M_{x0},\quad H_y=H_{{\rm app},y}-N_{yy}M_{y0};$$
$$H_z=H_{{\rm app},z}-N_{zz}M_{z0}=H_{{\rm app},z}-(1-N_{xx}-N_{yy})M_{z0}. \tag{22}$$

Therefore, if the in-plane demagnetizing factor increases, in order to achieve the same magnetic field inside the material, one needs to increase the applied field. In the same time, the out-of-plane demagnetizing field will decrease, which results in the decrease of the applied out-of-plane field. Immediately, one can connect this with the coercivity measurement of rough thin magnetic films. If we assume that during the thin-film formation, the film remains as a single domain structure and the magnetic energy is dominated by the magnet-static energy, then the actual coercivity of the film is fixed. Under this assumption, if the roughness of the film is changed, then the applied field corresponding to the real coercivity field also changes. According to Eq. (22), for the in-plane coercivity measurement, the apparent coercivity will change linearly with the in-plane demagnetizing factor. In other words, if the change of apparent coercivity has no relation to the demagnetizing factor, then the magnetization mechanism of the thin film may be different, i.e., the assumptions for a single domain and a dominate magnet-static energy are broken.

Connections with experiment: Experimentally the general trends for the magnetic thin films are that the apparent coercivity increases with film roughness,[5–10] which seems to agree with our above simple argument. In fact, the situation is more complicated: the increase of surface roughness does not guarantee the increase of the demagnetizing factor. In general one tends to use the interface width (root-mean square roughness) w to measure how rough the surface is: if w is large, then the surface is rougher. However, through the discussion in Sec. III, we have demonstrated that the demagnetizing factor depends not only on w but also on the film thickness d, the lateral correlation length ξ, and the roughness exponent α (if the surface is self-affine). Take an example of the noise-driven growth discussed in Sec. III A. We know from the dynamic scaling theory that the interface width grows as $w\propto t^{\beta}$, where in general $\beta>0$.[15] That is, with the increase of growth time, the surface becomes rougher. However, from our discussion in Sec. III A, the in-plane demagnetizing factor scales with the growth time as $N_{xx(yy)}\propto t^{2\beta-\beta/\alpha-1}$, where the exponent usually is negative. That is, the demagnetizing factor decreases with the growth time. This demonstrates that the increase of surface roughness (w) does not mean the increase of the demagnetizing factor. However, if the growth is in mound formation, as discussed in Sec. III B, the increase of roughness can indeed increase the demagnetizing factor. Therefore, the relation between the roughness and the demagnetizing factor is more dependent on the growth mechanism, or the detailed morphology of the surface; so does the apparent coercivity, given that the film is a single domain. Nonetheless, how does the detailed morphology of the surface affects the apparent coercivity was not considered in most experiments.[6–8,10] Only a few experiments relate the change in coercivity to the change of the interface width w. Recently, some detailed works have been performed.[5,9]

Experiments of Co films: In the following we shall discuss the connection of our theory and our experimental work. First, we examine the single rough boundary. For Co ultrathin films deposited on atomically smooth Cu substrate, Jiang *et al.* found that the apparent coercivity increases when the Co thickness increases from 1 to about 7 ML, and decreases slightly when Co grows beyond 7 ML thick.[5] In addition, they measured the detail surface morphology parameters (Table I in Ref. 5a) using high-resolution low-energy electron diffraction. One thing quite obvious is that the interface width w almost does not change for the thickness measured, but both the lateral correlation length ξ and the roughness exponent α have more dramatic change. From 3 to 25 ML, α decreases from 0.95 to 0.54, and ξ decreases from 285 to 94 Å. They used Schlömann's theory to estimate the in-plane demagnetizing factor, and concluded that the demagnetizing factor decreases as the film thickness increases.[5] However, the absolute value of the demagnetizing factor is quite small, which cannot contribute to the change of the coercivity. Using roughness data in Table I of Ref. 5(a), we calculated the demagnetizing factor of the ultrathin Co film as a function of the thickness using Eq. (6) and the result is plotted in Fig. 9. Except for thickness $d<10$ ML, the demagnetizing factor increases with the film thickness. The slow change of the demagnetizing factor in the small thickness regime is probably due to that the small roughness approximation ($w\ll d$) does not apply here. This trend of the demagnetizing factor as a function of film thickness is opposite to the behavior of the apparent coercivity, which suggests that the magnet-static energy may not play an important role in these ultrathin films. In fact, the absolute value of the demagnetizing factor is also quite small, which supports this point.

Finally, we discuss the double rough boundary case. A detailed experiment of Co films deposited on plasma etched Si(100) substrate was performed by Li *et al.*[9] The substrates were first plasma etched for various time periods, then about

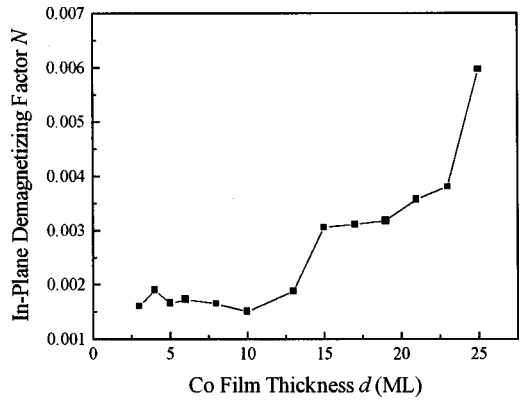

FIG. 9. The in-plane demagnetizing factor of the Co film as a function of thickness calculated using Eq. (6) from the data in Table I of Ref. 5(a).

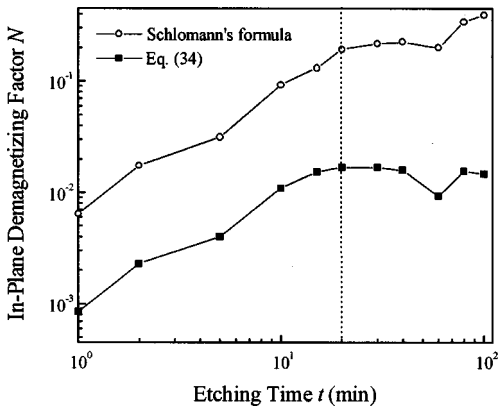

FIG. 10. Log-log plot of the in-plane demagnetizing factor as a function of the substrate etching time for the Co film using Eq. (20) and Schlömann's approximation.

970 Å Co films were deposited simultaneously on those substrates. Both substrate morphology before film deposition and the Co film morphology after deposition were measured by atomic-force microscopy, and the roughness parameters analyzed from height-height correlation functions were found to be correlated in-phase approximately. Therefore, Eq. (20) can be applied for this case. In Fig. 10 we plot the demagnetizing factors of the Co film as a function of the substrate etching time using both Eq. (20) and Schlömann's approximation. Clearly Schlömann's approximation gives a much larger demagnetizing factor and the demagnetizing factor increases with the etching time. However, Eq. (20) shows that the demagnetizing factor increases from 1 to 20 min, then decreases after that. In fact, for $t>30$ min, where the interface width $w>440$ Å, the small roughness perturbation is not valid because w is comparable to the thickness d. Going back to Eq. (5), we can actually expect a smaller N than the value calculated in Fig. 10. This result is consistent with the measured apparent coercivity, which shows a maximum around 20 min, and then decreases later in Ref. 9(b). However, the roughness-dependent demagnetizing factor cannot explain the behavior after 40 min.

VI. CONCLUSIONS

In conclusion, we studied in detail the influence of surface/interface roughness on the demagnetizing factor of a thin magnetic film for a wide range of rough morphologies. Moreover, the formalism was extended to account for films with film/substrate and film/vacuum rough interfaces by taking into account interface cross correlation effects. The following concludes our findings.

(a) For a film with a single self-affine rough boundary, the in-plane demagnetizing factor $N_{xx(yy)}$ is proportional to the interface width w square and to leading order is inversely proportional to the lateral correlation length ξ. The roughness exponent α is also shown to greatly affect $N_{xx(yy)}$ in such a manner that the demagnetizing factor can increase two orders of magnitude as α decreases from 1 to 0.

(b) For a film with a single mound boundary, $N_{xx(yy)}$ is inversely proportional to the apparent correlation length, and also depends on the ratio of the two different lateral lengths: the average mound separation and the randomness correlation length.

(c) An anisotropic surface morphology can induce anisotropic in-plane demagnetizing factors in such a manner that the demagnetizing anisotropy can be magnified drastically by morphological anisotropy. More precisely, the ratio of lateral demagnetizing factors N_{xx}/N_{yy} as a function of the lateral correlation length ratio ξ_x/ξ_y appeared to rotate by 90 degrees with respect to surface morphology anisotropy. The in-plane demagnetizing factor anisotropy and the lateral length scale anisotropy were found to obey the relation $N_{xx}/N_{yy} \propto (\xi_x/\xi_y)^{-1.7}$, implying that the slight anisotropy of surface morphology will be enlarged in the in-plane demagnetizing effect.

(d) Finally, we considered the case of films with two rough boundaries where we investigated how the cross correlation of the two rough boundaries affects the in-plane demagnetizing factors. The demagnetizing factor of in-phase boundaries is less than that of the out-of-phase boundaries. The thickness and correlation length dependence of the lateral demagnetizing factor $N_{xx(yy)}$ depends strongly on the corresponding roughness exponent. Indeed, for large roughness exponents α (=1), the demagnetizing factor $N_{xx(yy)}$ for the in-phase boundaries is significantly smaller than that for the out-of-phase boundaries. Moreover, the behavior of $N_{xx(yy)}$ versus d and ξ for the in-phase boundaries obviously deviates from the inversely proportional behavior with film thickness, instead $N_{xx(yy)}$ varies as $N_{xx} \propto d^{-1.1}$, and $N_{xx} \propto \xi^{-0.85}$. However, as roughness exponent α decreases, the $N_{xx(yy)}$ vs d and ξ behaviors for both in-phase and out-of-phase boundaries become similar and overlap with each other and the inverse dependence over d and ξ resumes. Connections with thin-film growth mechanisms were also explored and strongly influence roughness induced demagnetizing effect.

ACKNOWLEDGMENTS

This work was supported by the NSF. G.P. would like to acknowledge support from the Netherlands Institute for Metal Research.

APPENDIX A

Calculation of demagnetizing factors: In this section we explain briefly the algebra that leads to the final expressions for the demagnetizing factors; in-plane and out-of-plane. From Eqs. (1) and (2) we obtain the self-energy

$$\begin{aligned}
W_x &= -\frac{1}{2}M_{0x}\int d\mathbf{r}\int dz\,\frac{\partial \Phi_M}{\partial x}\left\{\theta\left(z+\frac{d}{2}-h_2(\mathbf{r})\right)-\theta\left(z-\frac{d}{2}-h_1(\mathbf{r})\right)\right\}\\
&= \frac{1}{2}M_{0x}\int d\mathbf{r}\left[\Phi_M\left(\mathbf{r},\frac{d}{2}+h_1\right)\frac{\partial h_1}{\partial x}-\Phi_M\left(\mathbf{r},-\frac{d}{2}+h_2\right)\frac{\partial h_2}{\partial x}\right]\\
&= \frac{1}{2}M_{0x}\int d\mathbf{r}\int d\mathbf{r}'\left\{\frac{(\partial h_1/\partial x')M_{0x}+(\partial h_1/\partial y')M_{0y}-M_{0z}}{\sqrt{(\mathbf{r}-\mathbf{r}')^2+[h_1(\mathbf{r})-h_1(\mathbf{r}')]^2}}-\frac{(\partial h_2/\partial x')M_{0x}+(\partial h_2/\partial y')M_{0y}-M_{0z}}{\sqrt{(\mathbf{r}-\mathbf{r}')^2+[d+h_1(\mathbf{r})-h_2(\mathbf{r}')]^2}}\right\}\frac{\partial h_1}{\partial x}\\
&\quad -\frac{1}{2}M_{0x}\int d\mathbf{r}\int d\mathbf{r}'\left\{\frac{(\partial h_1/\partial x')M_{0x}+(\partial h_1/\partial y')M_{0y}-M_{0z}}{\sqrt{(\mathbf{r}-\mathbf{r}')^2+[h_2(\mathbf{r})-h_1(\mathbf{r}')-d]^2}}-\frac{(\partial h_2/\partial x')M_{0x}+(\partial h_2/\partial y)M_{0y}-M_{0z}}{\sqrt{(\mathbf{r}-\mathbf{r}')^2+[h_2(\mathbf{r})-h_2(\mathbf{r}')]^2}}\right\}\frac{\partial h_2}{\partial x}.
\end{aligned} \tag{A1}$$

The expression for W_y is similar to W_x. For W_z, we have

$$\begin{aligned}
W_z &= -\frac{1}{2}M_{0z}\int d\mathbf{r}\int_{-d/2+h_2}^{d/2+h_1}dz\,\frac{\partial \Phi_M}{\partial z}=-\frac{1}{2}M_{0z}\int d\mathbf{r}\left[\Phi_M\left(\mathbf{r},\frac{d}{2}+h_1\right)-\Phi_M\left(\mathbf{r},-\frac{d}{2}+h_2\right)\right]\\
&= \frac{1}{2}M_{0z}\int d\mathbf{r}\int d\mathbf{r}'\left\{\frac{(\partial h_2/\partial x')M_{0x}+(\partial h_2/\partial y')M_{0y}-M_{0z}}{\sqrt{(\mathbf{r}-\mathbf{r}')^2+[d+h_1(\mathbf{r})-h_2(\mathbf{r}')]^2}}-\frac{(\partial h/\partial x')M_{0x}+(\partial h_1/\partial y')M_{0y}-M_{0z}}{\sqrt{(\mathbf{r}-\mathbf{r}')^2+[h_1(\mathbf{r})-h_1(\mathbf{r}')]^2}}\right\}\\
&\quad +\frac{1}{2}M_{0z}\int d\mathbf{r}\int d\mathbf{r}'\left\{\frac{(\partial h_1/\partial x')M_{0x}+(\partial h_1/\partial y')M_{0y}-M_{0z}}{\sqrt{(\mathbf{r}-\mathbf{r}')^2+[h_2(\mathbf{r})-h_1(\mathbf{r}')-d]^2}}-\frac{(\partial h_2/\partial x')M_{0x}+(\partial h_2/\partial y')M_{0y}-M_{0z}}{\sqrt{(\mathbf{r}-\mathbf{r}')^2+[h_2(\mathbf{r})-h_2(\mathbf{r}')]^2}}\right\}.
\end{aligned} \tag{A2}$$

Since $W=(4\pi dA/2)\mathbf{M}\cdot\vec{\mathbf{N}}\cdot\mathbf{M}$,[11] where A is the average flat surface area, we have

$$\begin{aligned}
N_{xx} &= \frac{1}{4\pi dA}\int d\mathbf{r}\int d\mathbf{r}'\left\{\frac{(\partial h_1/\partial x')(\partial h_1/\partial x)}{\sqrt{(\mathbf{r}-\mathbf{r}')^2+[h_1(\mathbf{r})-h_1(\mathbf{r}')]^2}}-\frac{(\partial h_2/\partial x')(\partial h_1/\partial x)}{\sqrt{(\mathbf{r}-\mathbf{r}')^2+[d+h_1(\mathbf{r})-h_2(\mathbf{r}')]^2}}\right.\\
&\quad \left.-\frac{(\partial h_1/\partial x')(\partial h_2/\partial x)}{\sqrt{(\mathbf{r}-\mathbf{r}')^2+[h_2(\mathbf{r})-h_1(\mathbf{r}')-d]^2}}+\frac{(\partial h_2/\partial x')(\partial h_2/\partial x)}{\sqrt{(\mathbf{r}-\mathbf{r}')^2+[h_2(\mathbf{r})-h_2(\mathbf{r}')]^2}}\right\},
\end{aligned} \tag{A3}$$

$$\begin{aligned}
N_{zz} &= \frac{1}{2\pi dA}\int d\mathbf{r}\int d\mathbf{r}'\left\{\frac{1}{\sqrt{(\mathbf{r}-\mathbf{r}')^2+[h_1(\mathbf{r})-h_1(\mathbf{r}')]^2}}-\frac{1}{\sqrt{(\mathbf{r}-\mathbf{r}')^2+[d+h_1(\mathbf{r})-h_2(\mathbf{r}')]^2}}\right.\\
&\quad \left.-\frac{1}{\sqrt{(\mathbf{r}-\mathbf{r}')^2+[h_2(\mathbf{r})-h_1(\mathbf{r}')-d]^2}}+\frac{1}{\sqrt{(\mathbf{r}-\mathbf{r}')^2+[h_2(\mathbf{r})-h_2(\mathbf{r}')]^2}}\right\}.
\end{aligned} \tag{A4}$$

Here N_{xx}, N_{yy}, and N_{zz} are the diagonal components of the demagnetizing tensor $\vec{\mathbf{N}}$. A similar calculation can be applied to the nondiagonal components N_{xy}, N_{yz}, and N_{zx}. If we assume the surface roughness w is much smaller than the film thickness $d(w\ll d)$, then the roughness can be treated as a small perturbation. In this limit the in-plane demagnetizing factor N_{xx} can be approximated as

$$N_{xx}\approx\frac{1}{4\pi dA}\int d\mathbf{r}\int d\mathbf{r}'\left\{\frac{(\partial h_1/\partial x')(\partial h_1/\partial x)+(\partial h_2/\partial x')(\partial h_2/\partial x)}{|\mathbf{r}-\mathbf{r}'|}-\frac{2(\partial h_2/\partial x')(\partial h_1/\partial x)}{\sqrt{(\mathbf{r}-\mathbf{r}')^2+d^2}}\right\}. \tag{A5}$$

Upon substitution of the Fourier transforms from Eqs. (2)–(4) we obtain

$$\int d\mathbf{r}\int d\mathbf{r}'\frac{\left\langle \frac{\partial h_i}{\partial x}\frac{\partial h_i}{\partial x'}\right\rangle}{|\mathbf{r}-\mathbf{r}'|}=-\int d\mathbf{r}\int d\mathbf{r}'\int d\mathbf{k}\int d\mathbf{k}'\frac{k_x^2}{|\mathbf{r}-\mathbf{r}'|}\langle\tilde{h}_i(\mathbf{k})\tilde{h}_i(\mathbf{k}')\rangle\exp(-i\mathbf{k}\cdot\mathbf{r}-i\mathbf{k}'\cdot\mathbf{r}')$$

$$=-\frac{(2\pi)^4}{A}\int d\mathbf{r}\int d\mathbf{r}'\int d\mathbf{k}\frac{k_x^2}{|\mathbf{r}-\mathbf{r}'|}\langle|\tilde{h}_i(\mathbf{k})|^2\rangle\exp[-i\mathbf{k}\cdot(\mathbf{r}-\mathbf{r}')]$$

$$=(2\pi)^5\int d\mathbf{k}\frac{k_x^2}{k}\langle|\tilde{h}_i(\mathbf{k})|^2\rangle \tag{A6}$$

and

$$\int d\mathbf{r}\int d\mathbf{r}'\frac{(\partial h_1/\partial x)(\partial h_2/\partial x')}{\sqrt{(\mathbf{r}-\mathbf{r}')^2+d^2}}=-\frac{(2\pi)^4}{A}\int d\mathbf{r}\int d\mathbf{r}'\int d\mathbf{k}\frac{k_x^2\langle\tilde{h}_1(\mathbf{k})\tilde{h}_2(-\mathbf{k})\rangle\exp[-i\mathbf{k}\cdot(\mathbf{r}-\mathbf{r}')]}{\sqrt{(\mathbf{r}-\mathbf{r}')^2+d^2}}$$

$$=(2\pi)^5\int d\mathbf{k}k_x^2\langle\tilde{h}_1(\mathbf{k})\tilde{h}_2(-\mathbf{k})\rangle\int_0^\infty dR\frac{RJ_0(kR)}{\sqrt{R^2+d^2}}$$

$$=(2\pi)^5\int d\mathbf{k}\frac{k_x^2}{k}e^{-dk}\langle\tilde{h}_1(\mathbf{k})\tilde{h}_2(-\mathbf{k})\rangle. \tag{A7}$$

Substituting Eq. (A6) and Eq. (A7) into Eq. (A5), we obtain the expression for Eq. (6).

APPENDIX B

In this appendix we consider a general case of the cross correlation between h_1 and h_2 due to dynamic roughening. We assume h_2 to be the initial height in a rough substrate and h_1 the growth front following certain growth mechanisms. The simplest case is to assume that the growth mechanism is linear. Then the equation of the growth front roughening can be written as

$$\frac{\partial h_1}{\partial t}=Lh_1+\eta, \tag{B1}$$

where L is the linear operator, and η is Gaussian white noise, satisfying the relations

$$\langle\eta(\mathbf{r},t)\rangle=0,$$

$$\langle\eta(\mathbf{r}_1,t_1)\eta(\mathbf{r}_2,t_2)\rangle=2D\delta(\mathbf{r}_1-\mathbf{r}_2)\delta(t_1-t_2). \tag{B2}$$

Performing a Fourier transform of Eq. (B1), one obtains the solution for h_1 in Fourier space[18]

$$\tilde{h}_1(\mathbf{k},t)=\int_0^t\tilde{\eta}(\mathbf{k},t')e^{\tilde{L}(\mathbf{k})(t-t')}dt'+\tilde{h}_2(\mathbf{k})e^{\tilde{L}(\mathbf{k})t}. \tag{B3}$$

Since $\langle\tilde{h}_2(\mathbf{k})\tilde{\eta}(\mathbf{k}',t)\rangle=0$, the cross correlation in k space can be written as

$$\langle\tilde{h}_1(\mathbf{k},t)\tilde{h}_2(\mathbf{k}')\rangle=\frac{A}{(2\pi)^5}e^{\tilde{L}(\mathbf{k})t}\langle|\tilde{h}_2(\mathbf{k})|^2\rangle\delta(\mathbf{k}+\mathbf{k}'). \tag{B4}$$

In addition,

$$\langle\tilde{h}_1(\mathbf{k},t)\tilde{h}_1(\mathbf{k}',t)\rangle=\frac{A}{(2\pi)^5}\left[e^{2\tilde{L}(\mathbf{k})t}\langle|\tilde{h}_2(\mathbf{k})|^2\rangle+D\frac{e^{2\tilde{L}(\mathbf{k})t}-1}{\tilde{L}(\mathbf{k})}\right]\delta(\mathbf{k}+\mathbf{k}'). \tag{B5}$$

For simplicity, we adapt the linear model discussed in Ref. 18, the linear operator L has the form

$$L=\pm\nu\nabla^2-\kappa\nabla^4, \tag{B6}$$

or alternatively in k space

$$\tilde{L}(\mathbf{k})=\mp\nu k^2-\kappa k^4. \tag{B7}$$

κ is proportional to the surface diffusion coefficient. For $+\nu$ we have the case of stable growth (noise induced roughening) with ν proportional to the surface tension coefficient. For $-\nu$ we have the case of unstable growth (unstable mound formation) due to the diffusion (Schwoebel) barrier. Therefore, we obtain

$$\langle\tilde{h}_1(\mathbf{k},t)\tilde{h}_2(\mathbf{k}')\rangle=\frac{A}{(2\pi)^5}e^{(\mp\nu k^2-\kappa k^4)t}\langle|\tilde{h}_2(\mathbf{k})|^2\rangle\delta(\mathbf{k}+\mathbf{k}'), \tag{B8}$$

and

$$\langle\tilde{h}_1(\mathbf{k},t)\tilde{h}_1(\mathbf{k}',t)\rangle=\frac{A}{(2\pi)^5}\left[e^{2(\mp\nu k^2-\kappa k^4)t}\langle|\tilde{h}_2(\mathbf{k})|^2\rangle+D\frac{e^{2(\mp\nu k^2-xk^4)t}-1}{\mp\nu k^2-\kappa k^4}\right]\delta(\mathbf{k}+\mathbf{k}'). \tag{B9}$$

[1] *Ultrathin Magnetic Structures I and II*, edited by J. A. C. Bland and B. Heinrich (Springer, New York, 1994).
[2] C. H. Chang and M. H. Kryder, J. Appl. Phys. **75**, 6864 (1994).
[3] P. Bruno, G. Bayureuther, P. Beauvillain, C. Chappert, G. Lugert, D. Renard, J. P. Renard, and J. Seiden, J. Appl. Phys. **68**, 5759 (1990).
[4] J. Barnas and Y. Bruynseraede, Europhys. Lett. **32**, 167 (1995); Phys. Rev. B **53**, 5449 (1996); J. Barnas and G. Palasantzas, J. Appl. Phys. **82**, 3950 (1997); S. Zhang and P. M. Levy, Phys. Rev. Lett. **77**, 916 (1996).
[5] (a) Q. Jiang, H.-N. Yang, and G.-C. Wang, Surf. Sci. **373**, 181 (1997); (b) J. Vac. Sci. Technol. B **14**, 3180 (1996).
[6] S. Vilain, J. Ebothe, and M. Troyon, J. Magn. Magn. Mater. **157**, 274 (1996).
[7] V. I. Malyutin, V. E. Osukhovskii, Yu. D. Vorobiev, A. G. Shishkov, and V. V. Yudin, Phys. Status Solidi A **65**, 45 (1981).
[8] J. W. Freeland, K. Bussmann, P. Lubitz, Y. U. Idzerda, and C.-C. Kao, Appl. Phys. Lett. **73**, 2206 (1998).
[9] (a) M. Li, G.-C. Wang, and H.-G. Min, J. Appl. Phys. **83**, 5313 (1998); (b) M. Li, Y.-P. Zhao, G.-C. Wang, and H.-G. Min, *ibid.* **83**, 6287 (1998).
[10] J.-H. Kim and S.-C. Shin, Jpn. J. Appl. Phys., Part 1 **35**, 342 (1996).
[11] E. Schlömann, J. Appl. Phys. **41**, 1617 (1970).
[12] A. Moschel, R. A. Hyman, A. Zangwill, and M. D. Stiles, Phys. Rev. Lett. **77**, 3653 (1996).
[13] G. Palasantzas, J. Appl. Phys. (to be published 1 August 1999).
[14] J. D. Jackson, *Classical Electrodynamics*, 2nd ed. (Wiley New York, 1975), p. 194.
[15] For a review, see *Dynamics of Fractal Surfaces*, edited by F. Family and T. Vicsek (World-Scientific, Singapore, 1990); A.-L. Barabási and H. E. Stanley, *Fractal Concepts in Surface Growth* (Cambridge University Press, New York, 1995).
[16] J. Villian, J. Phys. I **1**, 19 (1991); M. D. Johnson, C. Orme, A. W. Hunt, D. Graff, J. Sudijono, L. M. Sander, and B. G. Orr, Phys. Rev. Lett. **72**, 116 (1994); M. Siegert and M. Plischke, *ibid.* **73**, 1517 (1994).
[17] R. P. U. Karunasiri, R. Bruinsma, and J. Rudnick, Phys. Rev. Lett. **62**, 788 (1989); J. H. Yao and H. Guo, Phys. Rev. E **47**, 1007 (1993).
[18] Y.-P. Zhao, H.-N. Yang, G.-C. Wang, and T.-M. Lu, Phys. Rev. B **57**, 1922 (1998), and references therein.
[19] Y.-P. Zhao, G.-C. Wang, and T.-M. Lu, Phys. Rev. B **58**, 13 909 (1998).
[20] Y.-P. Zhao, G.-C. Wang, and T.-M. Lu, Phys. Rev. B **58**, 7300 (1998).
[21] G. Palasantzas, Phys. Rev. B **48**, 14 472 (1993); Phys. Rev. E **49**, 1740 (1994).
[22] I. S. Gradshteyn and I. M. Ryzhik, *Table of Integrals, Series, and Products*, 5th ed. (Academic, Boston, 1994).